The results obtained in Ref. [42] demonstrated that employing NNs makes it possible to extend the capabilities of distributed IMSs because of using the entire transfer OFML characteristic, and not just its linear portion. This is achieved through the optimal combination of the conjugate-gradient, gradient descent, and thermal annealing methods in the course of perceptron learning [42–44] and the use of the transfer function of the form $f(\ldots) = \tanh(\ldots)$.

The elaborated notions of NN structure and learning methods were realized in Refs [41, 43] in the development of an optoelectronic NN with a holographic coupling matrix, which enables a real-time reconstruction of the PF parameter distribution in the IMS with an accuracy of 6 to 20%, whose operation is illustrated in Fig. 3.

5. Conclusions

The aim of this report was to outline the results that have led to advances in a new area of physical instrument making, which emerged at the interface between several modern fields of knowledge, namely, laser physics, optoelectronics, and artificial intelligence. The emergence of this area is associated with an impetuous introduction into practice of processes and objects which should be monitored and controlled in real time. These problems bring to the fore the necessity to develop high-precision, high-reliable, and fast-response measuring devices with a capacity to adapt to specific conditions of their operating, learning, and solving problems when the data obtained are deficient, and which also have the capacity for pattern recognition and situation prediction. In the future, the problems of development of the physical principles and production technologies of adaptive optoelectronic IMSs should therefore become central to their practical application.

References

1. Kersey A D *Opt. Fiber Technol.* **2** 291 (1996)
2. Butusov M M et al. *Volokonnaya Optika i Priborostroenie* (Fiber Optics and Instrument Making) (Ed. M M Butusov) (Leningrad: Mashinostroenie, 1987)
3. Kul'chin Yu N *Raspredelennye Volokonno-Opticheskie Izmeritel'nye Sistemy* (Distributed Optical Fiber Measuring Systems) (Moscow: Fizmatlit, 2001)
4. Pinchevskiĭ A D *Izmerit. Tekh.* (8) 3 (1991) [*Meas. Tech.* **34** 741 (1991)]
5. Ivanov V N, Kavalerov G I *Izmerit. Tekh.* (10) 8 (1991) [*Meas. Tech.* **34** 978 (1991)]
6. Malekhanov A I *Izv. Vyssh. Uchebn. Zaved. Radiofiz.* **31** 1388 (1988)
7. Kul'chin Yu N et al. *Kvantovaya Elektron.* **20** 513 (1993) [*Quantum Electron.* **23** 444 (1993)]
8. Kul'chin Yu N, Vitrik O B *Izmerit. Tekh.* (3) 24 (1999)
9. Kul'chin Yu N et al. *Izmerit. Tekh.* (3) 32 (1995) [*Meas. Tech.* **38** 304 (1995)]
10. Vitrik O B et al., in *Distributed and Multiplexed Fiber Optic Sensor IV* (Proc. SPIE, Vol. 2294, Eds A D Kersey, J P Dakin) (San Diego: SPIE, 1994) p. 165
11. Kotov O I et al. *Pis'ma Zh. Tekh. Fiz.* **16** (2) 90 (1990) [*Sov. Tech. Phys. Lett.* **16** 81 (1990)]
12. Ginevskiĭ S P et al. *Kvantovaya Elektron.* **22** 1013 (1995) [*Quantum Electron.* **25** 978 (1995)]
13. Kul'chin Yu N et al. *Kvantovaya Elektron.* **22** 1009 (1995) [*Quantum Electron.* **25** 974 (1995)]
14. Kul'chin Yu N et al. *Kvantovaya Elektron.* **24** 467 (1997) [*Quantum Electron.* **27** 455 (1997)]
15. Kulchin Yu N et al. *Fiber Integrated Opt.* **17** 75 (1998)
16. Kul'chin Yu N et al. *Izmerit. Tekh.* (6) 21 (1999) [*Meas. Tech.* **42** 541 (1999)]
17. Natterer F *The Mathematics of Computerized Tomography* (Stuttgart: B.G. Teubner, 1986) [Translated into Russian (Moscow: Mir, 1990)]
18. Tikhonov A N, Arsenin V Ya *Metody Resheniya Nekorrektnykh Zadach* (Solutions of Ill-Posed Problems) 2nd ed. (Moscow: Nauka, 1979) [Translated into English (New York: Halsted Press, 1977)]
19. Bykovskiĭ Yu A et al. *Kvantovaya Elektron.* **17** 1080 (1990) [*Sov. J. Quantum Electron.* **20** 996 (1990)]
20. Kul'chin Yu N, Obukh V F *Kvantovaya Elektron.* **13** 650 (1986) [*Sov. J. Quantum Electron.* **16** 424 (1986)]
21. Bykovskiĭ Yu A, Vitrik O B, Kul'chin Yu N *Kvantovaya Elektron.* **17** 1377 (1990) [*Sov. J. Quantum Electron.* **20** 1288 (1990)]
22. Bykovskiĭ Yu A et al. *Kvantovaya Elektron.* **17** 95 (1990) [*Sov. J. Quantum Electron.* **20** 83 (1990)]
23. Kamshilin A A, Jaaskelainen T, Kulchin Yu N *Appl. Phys. Lett.* **73** 705 (1998)
24. Kulchin Yu N et al., in *Distributed Fiber Optical Sensors and Measuring Networks* (Proc. SPIE, Vol. 4357, Ed. Yu N Kulchin) (Bellingham, Wash.: SPIE, 2001) p. 130
25. Kulchin Yu N, Romashko R V, Kamenev O T, in *Fundamental Problems of Optoelectronics and Microelectronics* (Proc. SPIE, Vol. 5129, Eds Yu N Kulchin, O B Vitrik) (Bellingham, Wash.: SPIE, 2003) p. 168
26. Kamshilin A A et al. *Appl. Phys. B: Laser Opt.* **68** 1031 (1999)
27. Borodin M V et al. *Izv. Vyssh. Uchebn. Zaved. Fiz.* **44** (10) 38 (2001) [*Russ. Phys. J.* **44** 1050 (2001)]
28. Feinberg J *J. Opt. Soc. Am.* **72** 46 (1982)
29. Voronov V V et al. *Kvantovaya Elektron.* **7** 2313 (1980) [*Sov. J. Quantum Electron.* **10** 1346 (1980)]
30. Xie P et al. *J. Appl. Phys.* **74** 813 (1993)
31. Kamshilin A A et al. *Opt. Lett.* **24** 832 (1999)
32. Kamshilin A A et al. *Appl. Phys. Lett.* **74** 2575 (1999)
33. Cronin-Golomb M, Yariv A *J. Appl. Phys.* **57** 4906 (1985)
34. Arizmendi L, Cabrera J M, Agullo-Lopez F *Int. J. Optoelectron.* **7** 149 (1992)
35. Kobozev O et al. *J. Opt. A: Pure Appl. Opt.* **3** L9 (2001)
36. Kul'chin Yu N et al. *Pis'ma Zh. Tekh. Fiz.* **26** (12) 23 (2000) [*Tech. Phys. Lett.* **26** 505 (2000)]
37. Kulchin Yu N et al. *Opt. Eng.* **36** 1494 (1997)
38. Kul'chin Yu N, Kamenev O T, in *Kibernetika i Vuz* (Cybernetics and Institute of Higher Education) Issue 28 (Tomsk: TPU, 1994) p. 3
39. Kulchin Yu N et al. *Opt. Memory Neural Networks* **6** 149 (1997)
40. Kulchin Yu N, Kamenev O T *Laser Biology* **4** 625 (1995)
41. Kul'chin Yu N, Denisov I V, Kamenev O T *Pis'ma Zh. Tekh. Fiz.* **25** (6) 65 (1999) [*Tech. Phys. Lett.* **25** 235 (1999)]
42. Kulchin Yu N, Panov A V *Pacific Sci. Rev.* **3** 1 (2001)
43. Kulchin Yu N et al., in *Fundamental Problems of Optoelectronics and Microelectronics* (Proc. SPIE, Vol. 5129, Eds Yu N Kulchin, O B Vitrik) (Bellingham, Wash.: SPIE, 2003) p. 162
44. Kulchin Yu N et al., in *Fundamental Problems of Optoelectronics and Microelectronics* (Proc. SPIE, Vol. 5129, Eds Yu N Kulchin, O B Vitrik) (Bellingham, Wash.: SPIE, 2003) p. 176
45. Mikaelian A L et al. *Opt. Memory Neural Networks* **1** 7 (1992)
46. Wasserman Ph D *Neural Computing: Theory and Practice* (New York: Van Nostrand Reinhold, 1989) [Translated into Russian (Moscow: Mir, 1992)]

PACS numbers: **42.62.–b**, 87.56.By, 87.59.Dj
DOI: 10.1070/PU2003v046n08ABEH001655

Laser electron-beam X-ray source for medical applications

E G Bessonov, A V Vinogradov, M V Gorbunkov, A G Tur'yanskiĭ, R M Feshchenko, Yu V Shabalin

1. Introduction

At present, a rich variety of diagnostic procedures and interventions in cardiology, neurosurgery, etc. are performed with X-ray monitoring. In so doing, X-ray tubes remain the

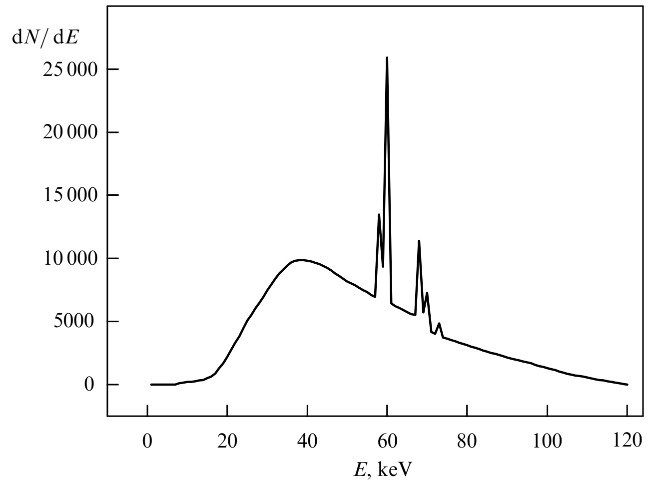

Figure 1. Spectrum of a medical X-ray tube with a tungsten anode at 120 kV according to the tabular data of Ref. [17].

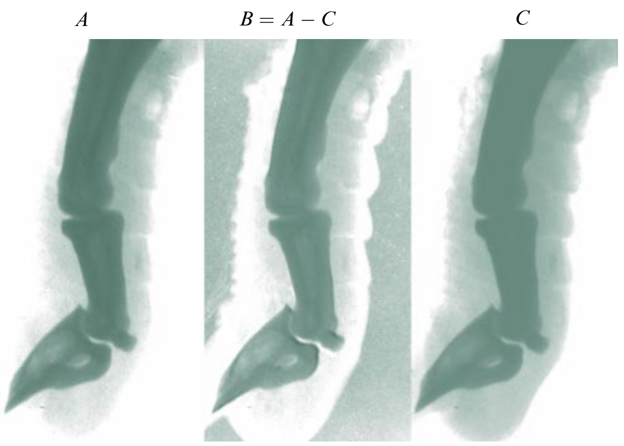

Figure 2. Image of a toe of a rat's forefoot in the polychromatic spectrum of an X-ray tube with a copper anode: A, C — standard projections obtained respectively for a voltage of 21 kV with a Ni filter, and 16 kV without a filter, and B — difference $A-C$ of the images.

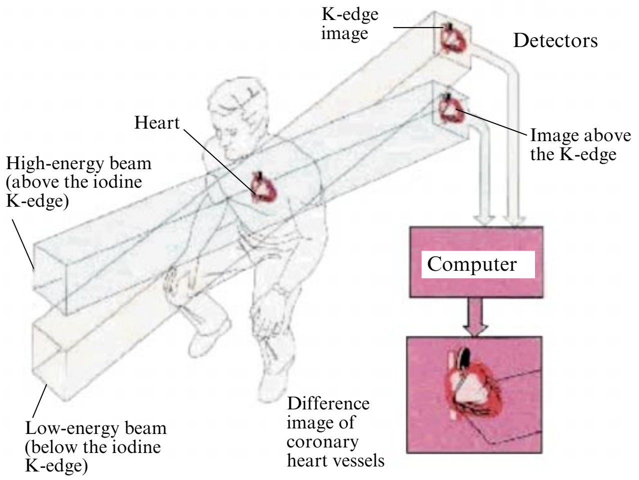

Figure 3. General view of the angiographic synchrotron channel [22].

only radiation source employed in practical medicine (to say nothing of radioisotope diagnostics). They possess a polychromatic spectrum (Fig. 1). It is well known that harnessing monochromatic and quasi-monochromatic beams allows a substantial reduction of irradiation dose and permits, in combination with techniques of image subtraction at the K-edge of the contrast element (iodine, as a rule), the attainment of a significant image quality (contrast) improvement for the organs under investigation or operation. Figure 2 shows the result of spectrum modification with subsequent image subtraction through the example of a rat's toe. We emphasize that the modified spectrum in this case is, like the initial one, polychromatic with some prevalence of the photons with energies $\hbar\omega \leqslant 8$ keV (below the absorption edge of the nickel filter). The subtraction of monochromatic images obtained at energies immediately below and above the absorption edge of the contrast material should be most advantageous [1].

We discuss this issue in greater detail through the example of coronary angiography (the main diagnostic tool of coronary angioplasty) — a relatively new and rapidly progressing method for treating myocardial ischemia. In 1994, coronary angioplasty interventions outnumbered coronary artery bypass grafting operations for the first time in 12 years [2]. Their cost amounts to billions of dollars. In coronary angiography, the images of blood vessels are produced due to the introduction of a contrast material with the aid of a catheter directly into the region under investigation in the vicinity of the heart. The results of such an examination underlie the conclusion about the necessity of treatment, intervention, or an operation. One of the reasons retarding wider dissemination of the method as well as its mass application for diagnosing myocardial ischemia and checking up on the state of blood vessels (scanning) of inhabitants is harmful side factors. Among them are significant irradiation doses received by patients and physicians, hazards associated with the introduction of the catheter, the injurious effect of the contrast material on human health, etc. During the last 15 years, a substantial effort has therefore been mounted to develop an alternative direction involving the production of two monochromatic images at the boundaries of the iodine absorption edge with subsequent computer processing. In this method, the increase in sensitivity to the presence of iodine will enable the physician to work at very low densities of the contrast material and introduce it by intravenous injections, in lieu of catheterization. The starting point of this approach is the availability of a monochromatic source with photon energies $\hbar\omega \approx 33$ keV (the abrupt change in iodine absorption). In principle, it can be developed on the base of an X-ray tube and crystal monochromators. However, the thus produced photon flux would be too low, eliminating the possibility of any clinical use or tests. The acceptable flux level is provided by synchrotron radiation [3]. In this connection, special-purpose angiography channels (see Fig. 3) were built at several modern synchrotrons [4–8]. Examinations by two-wave method were conducted on hundreds of patients to bear out the feasibility of coronary angiography without catheterization. However, it is still too early to discuss its practical application owing to the large dimensions of the facilities and their high cost, for the case in point is synchrotrons with energies of several gigaelectronvolts and ring diameters of the order of 20 m [1].

An alternative approach was proposed by the authors of Ref. [9], who reported experiments on phantoms with the aim of investigating the feasibility of two-wave coronary angiography reliant on a laser plasma X-ray source. The laser pulse energy was equal to 0.8 J for a pulse duration 150 and 400 fs and a repetition rate of 0.02 Hz, a focal spot measuring 5×5 μm, and a peak energy flux density of $\sim 10^{19}$ W cm^{-2}. According to the estimates reported by Krol et al. [9], the practical employment of a laser plasma radiation source in two-wave coronary angiography would require a laser with similar pulse parameters and an average power of 2–10 kW, where the main problem of laser plasma angiography is likely to lie.

2. Source parameters

Our work is also concerned with laser angiography, but on the basis of Compton backscattering of high-power laser radiation from relativistic electrons. This effect was first observed by Kulikov et al. [10] and the idea of harnessing it in medicine was discussed by Huang and Ruth [11]. We consider the interaction of pulse-periodic laser radiation with electron bunches of the storage ring, the repetition rate of laser pulses being coincided with the electron orbiting frequency. We will determine first the parameters of the laser and storage ring, required for the generation of a sufficiently intense beam of X-ray photons near the iodine absorption K-edge with $\hbar\omega \approx 33$ keV. In a head-on collision (see Fig. 4), the scattered X-ray photon frequency ω is related to the laser photon frequency through the expression

$$\hbar\omega = 4\gamma^2 \hbar\omega_{\mathrm{L}} \,, \tag{1}$$

where $\gamma = E_{\mathrm{e}}/mc^2$ is the relativistic factor, and E_{e} is the electron energy. For a laser with $\hbar\omega_{\mathrm{L}} = 1$ eV we obtain $\gamma = 91$ and $E_{\mathrm{e}} = 46$ MeV. The scattered radiation spectrum is depicted in Fig. 5, together with the iodine absorption cross section. The radiation is collimated in forward direction with an rms angle $\sim 1/\gamma \approx 10^{-2}$.

The relatively low electron energy allows us to orient ourselves to a compact storage ring with an orbit radius $R \sim 1$ m and an electron orbiting period $T = 20$ ns, which corresponds to a laser pulse repetition rate of 50 MHz.

Figure 4. Compton scattering from relativistic electrons.

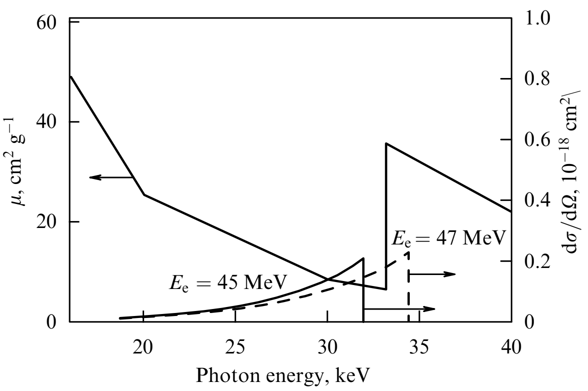

Figure 5. Mass absorption cross section μ of iodine and differential cross section $d\sigma/d\Omega$ for Compton scattering of laser radiation for two electron energies.

The average X-ray radiation flux arising in the Compton scattering can be represented as

$$\Phi = n_{\mathrm{e}}\sigma l \Phi_{\mathrm{L}} = N_{\mathrm{e}} \frac{\sigma}{s} \Phi_{\mathrm{L}} \,, \tag{2}$$

where Φ is the X-ray (Compton) photon flux measured in s^{-1}, Φ_{L} is the laser photon flux in s^{-1}, $\sigma = 6.6 \times 10^{-25}$ cm^2 is the Thomson cross section, n_{e} is the electron number density in the bunch, l is the bunch length, s is the cross-sectional area of the bunch, $N_{\mathrm{e}} = JT/e$ is the total number of electrons in the bunch, and J is the storage ring current.

The laser power required to attain the X-ray flux Φ can be represented, in view of formula (2), as follows

$$P_{\mathrm{L}} = sI_{\mathrm{L}} \,, \qquad I_{\mathrm{L}} = \frac{\Phi\hbar\omega_{\mathrm{L}}}{\sigma N_{\mathrm{e}}} \,. \tag{3}$$

In particular, proceeding from the X-ray flux $\Phi = 2 \times 10^{14}$ s^{-1} required for angiography [11] and the accelerator parameters

$$R = 1 \text{ m}\,, \qquad T = 20 \text{ ns}\,, \qquad J = 0.1 \text{ A}\,,$$
$$N_{\mathrm{e}} = 1.25 \times 10^{10} \text{ cm}^{-3} \,, \tag{4}$$

we find the energy flux density of the laser radiation interacting with the electron bunch:

$$I_{\mathrm{L}} = 4 \times 10^9 \text{ W cm}^{-2} \,. \tag{5}$$

The average laser power P_{L} and the pulse energy ε_{L} are compiled below in Table 1 for two realistic values of electron bunch diameter $s^{1/2}$ and a repetition rate of 50 MHz.

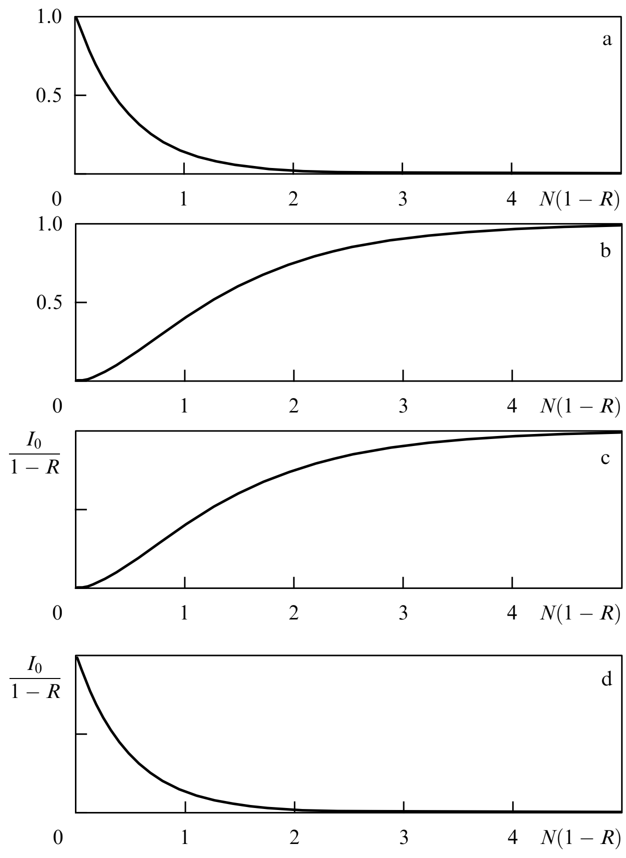

Figure 6. Transient processes in a Fabry–Perot cavity: (a) attaining of the cavity reflectivity; (b) attaining of the cavity transmittance; (c) attaining of radiation power inside the cavity, and (d) damping of the intracavity power upon removal of the external field (R is the reflectivity of both mirrors, N is the number of cavity go-rounds, and I_0 is the incident wave intensity).

Table 1

$s^{1/2}$, μm	30	100
$P_L = sI_L$, kW	40	400
$\varepsilon_L = P_L T$, mJ	0.8	8

Since the parameters of the laser pulse change only slightly in each scattering event, to improve the interaction efficiency there is good reason to take advantage of a Fabry–Perot cavity with high-reflectivity (R) mirrors. In this case, the above radiation energy parameters pertain to the laser beam inside the cavity. Outside the cavity they are $(1-R)^{-1}$ times smaller. For $R = 0.999$, in particular, a laser with an average output power of 40–400 W is required, according to the data in Table 1.

The cavity length should be matched with the perimeter of the electron orbit and, therefore, be equal to 3 m. Estimates show that the average radiation load on the cavity mirrors in this case is equal to 2–200 kW cm^{-2}, and the pulsed load to 0.04–4 mJ cm^{-2}. There exist optical materials with such a radiation resistance; however, it is well to bear in mind that the case in point is high-reflectivity cavity mirrors.

3. Discussion

To efficiently interact, the electron bunch, on the one hand, should be shorter than the waist region of the laser beam, in which the high intensity of laser radiation is produced. On the other hand, the laser pulse duration should not exceed the duration of the electron bunch. For a diffraction-limited laser beam, the length of the waist region equals s/λ (where λ is the wavelength) and the laser pulse duration therefore lies in the picosecond–femtosecond range. A diode-pumped ytterbium laser [12] approximates most closely the requirements formulated above. Its average power is equal to 60 W, the repetition rate to 34.3 MHz, the pulse duration to 0.81 ps, and the wavelength to 1.03 μm.

In the previous section, the effect of laser radiation on the dynamics of the electron beam in the storage ring was neglected. The discussion of this issue is being continued in the scientific literature [11, 13–15], and it seems likely that the issue will yet call for experimental investigation. In the pursuance of these experiments, the employment of a high-Q cavity is not a necessity and in some cases is even undesirable: the inertial properties inherent in the cavity would limit the turn-on and turn-off rates of its field and hence the possibilities for investigating the transient processes in the storage ring. This inertia is characterized by the number of passages N required for cavity field settling. The relaxation of reflectivity, transmittance, and intracavity power to equilibrium magnitudes is illustrated in Fig. 6. It can be shown that the time the stored energy takes to attain the 0.9 level of the steady-state value is $T \ln 20/(1-R)$, where R is the reflectivity of cavity mirrors, and T is the cavity go-round time. The damping of intracavity power and the decrease of reflectivity to the 0.1 level during relaxation take place in a time $0.5T \ln 10/(1-R)$.

The foregoing suggests that there is good reason to employ a radiation source which generates trains of a rather large and controllable (from 10^2 to 10^5) number of subpico-

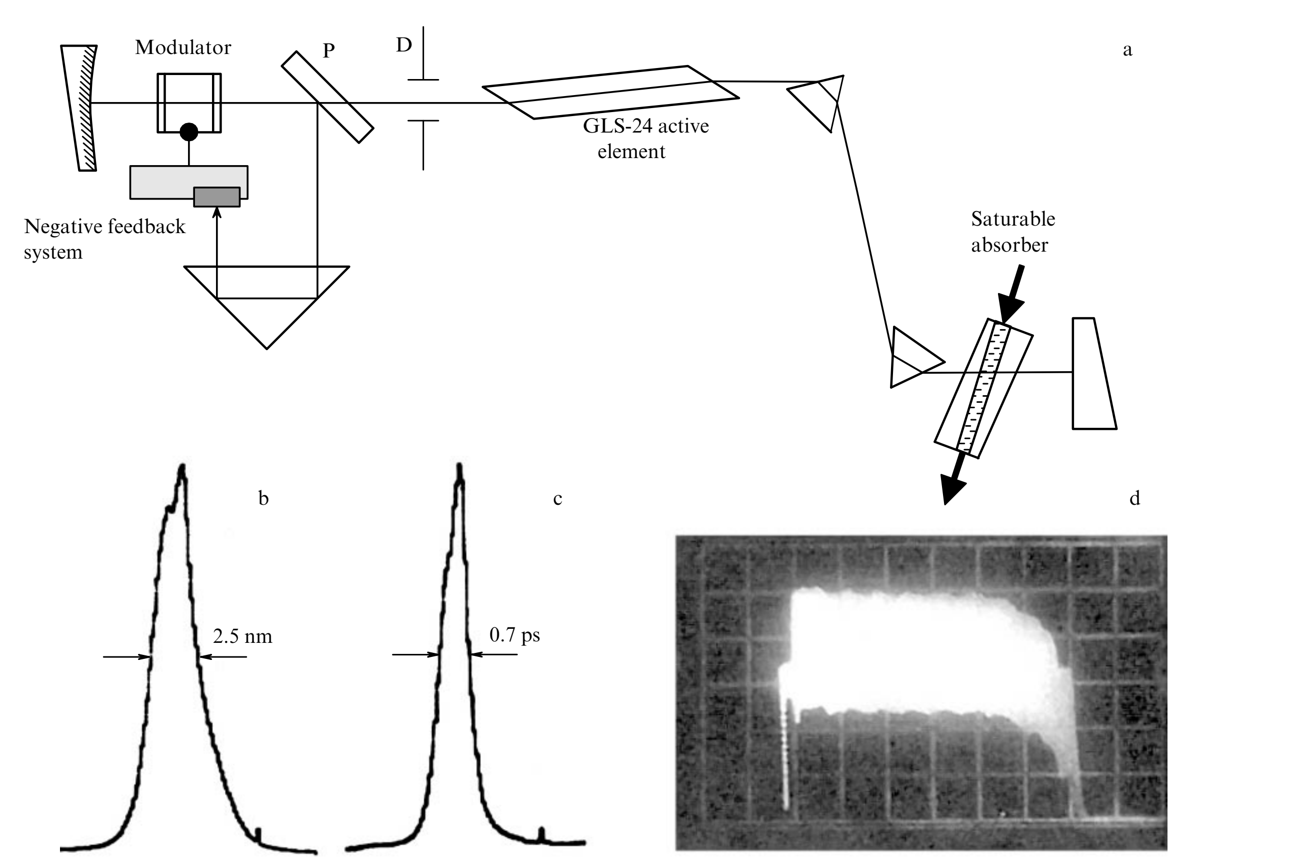

Figure 7. Subpicosecond phosphate-glass laser (the pulse train duration is 50–200 μs, the number of pulses $5\times10^3-2\times10^4$, the pulse duration 0.7 ps, the single-pulse energy 0.1–1 μJ): (a) schematic of the laser; (b) spectrum; (c) pulse correlation function, and (d) envelope of the pulse train (the time scale is 10 μs per division).

second laser pulses with a constant amplitude for investigating the interaction of laser and electron beams. A phosphate-glass laser of this type was developed in the P N Lebedev Physics Institute, Russian Academy of Sciences. The radiation stabilization and the generation of constant-amplitude subpicosecond laser pulses are attained through the use of an external optoelectronic negative-feedback system [16]. Schematic of the laser and its parameters are given in Fig. 7. The energy of a single pulse ranges from 0.1 to 1 μJ. Reaching the parameters specified in Section 2 requires multiplication by a factor of $10^3 - 10^4$; in this case, the total pulse train energy will be as high as 10 – 100 J, which appears to be quite realistic. In this case, the X-ray pulse train will contain $\sim 10^{11}$ photons, which will make it possible to record high-contrast images with up to 10^6 pixels in a time $\sim$ 1 ms.

4. Conclusions

Hence, state-of-the-art laser and accelerator technologies allow us to raise the question of the development of qualitatively new means of X-ray diagnostics, which can find application in different fields of medicine. In essence, the employment of a laser in lieu of magnetic undulator systems enables us to reduce the energy and dimensions of electron storage rings which generate X-ray radiation. The prospect of elaborating compact laser electron-beam X-ray sources attracts the attention of many scientific groups [18 – 21] worldwide due to the indisputable advantages over both X-ray tubes and synchrotrons. Among the applications, the emphasis is put on medicine, though others exist in non-destructive testing and security systems. The highly practical significance of these fields and the growing demand for new equipment are good spurs for the development of laser electron-beam X-ray radiation sources.

The authors express their appreciation to O N Krokhin, I G Zubarev, A N Lebedev, I A Artyukov, V I Panteleev, S V Savel'ev, S I Fedotov, and V I Shvedunov for their helpful discussions.

References

1. Ando M, Uyama C (Eds) *Medical Applications of Synchrotron Radiation* (Tokyo: Springer-Verlag, 1998)
2. Babunashvili A M, Rabkin I Kh, Ivanov V A *Koronarnaya Angioplastika* (Coronary Angioplasty) (Moscow: ASV, 1996)
3. Rubinstein E et al. *Proc. Natl. Acad. Sci. USA* **83** 9724 (1986)
4. Dolbnya I P et al. *Phys. Medica* **VI** (3 – 4) 313 (1990)
5. Kondratyev V I et al., in *Medical Applications of Synchrotron Radiation* (Eds M Ando, C Uyama) (Tokyo: Springer-Verlag, 1998) p. 29
6. Dix W-R et al., in *Intravenous Coronary Angiography with Synchrotron Radiation: Proc. of the 15th Intern. Congress and Exhibition CARS, 2001* (Intern. Congress Series, No. 1230) (Boston: Elsevier, 2001) p. 930
7. Elleaume H et al. *Phys. Med. Biol.* **45** L39 (2000)
8. Mori H et al. *Radiology* **201** 173 (1996)
9. Krol A et al. *Proc. SPIE* **4504** 227 (2001)
10. Kulikov O F et al. *Zh. Eksp. Teor. Fiz.* **47** 1591 (1964) [*Sov. Phys. JETP* **20** 1069 (1965)]
11. Huang Z, Ruth R D *Phys. Rev. Lett.* **80** 976 (1998)
12. Innerhofer E et al. *Opt. Lett.* **28** 367 (2003)
13. Huang Z, in *The Physics of High Brightness Beams: Proc. of the 2nd ICFA Advanced Accelerator Workshop* (Eds J Rosenzweig, L Serafini) (Singapore: World Scientific, 2000) p. 152
14. Bessonov E G, in *Proc. of the 18th Advanced ICFA Beam Dynamics Workshop on Quantum Aspects of Beam Physics, Capri, Italy, Oct. 15 – 20, 2000* (Ed. P Chen) (Singapore: World Scientific, 2002) p. 113
15. Bessonov E G, physics/0202040
16. Gorbunkov M V, Vorchik D B, in *Conf. on Lasers and Electro-Optics/Europe, CLEO/Europe'96, Sept. 8 – 13, 1996, Hamburg, Germany*, Technical Digest, p. 282
17. Vasil'ev V N et al. *Spektry Izlucheniya Rentgenovskikh Ustanovok* (Emission Spectra of X-Ray Facilities) (Moscow: Energoatomizdat, 1990)
18. Nakajima K, in *Advanced Accelerator Concepts: 8th Workshop, Baltimore, Maryland, July 1998* (AIP Conf. Proc., Vol. 472, Eds W Lawson, C Bellamy, D F Brosius) (Woodbury, NY: American Institute of Physics, 1999) p. 280
19. Litvinenko V N, Shevchenko O A, Mikhailov S F, in *Free Electron Lasers 2001: Proc. of the 23rd Intern. Free Electron Laser Conf. and the 8th FEL Users Workshop, Darmstadt, Germany, Aug. 20 – 24, 2001* (Eds M Brunken, H Genz, A Richter) (Boston: Elsevier, 2002) p. II-63
20. Agafonov A V et al. "Development of an advanced X-ray generator based on Compton back-scattering", A Proposal for Science for Peace Sub-Programme of NATO, Problems of Atomic Science and Technology (Ser. Nuclear Physics Investigations, No. 1) (2001) p. 126
21. Bessonov E G, Vinogradov A V, Tur'yanskiĭ A G *Prib. Tekh. Eksp.* (5) 142 (2002) [*Instrum. Exp. Tech.* **45** 718 (2002)]
22. Baghiryan M "Synchrotron radiation and applications", ASLS-CANDLE 02-012 (2002); http://www.candle.am/Public_reports/In_report/r_02_012.pdf

PACS numbers: 04.80.Nn, **98.80.–k**
DOI: 10.1070/PU2003v046n08ABEH001656

Cosmological model and universe structure formation

V N Lukash

The development, on the one hand, of new methods and technologies of measuring the anisotropy and polarization of relict radiation and, on the other hand, the elaboration of maps of large-scale visible-matter distribution in the Universe have led to the experimental determination of the cosmological model, which physicists and astronomers of the 20th century could only dream of. For the first time, the spatial spectrum of primary cosmological density perturbations has been measured on scales of length ranging from clusters ($\sim$ 10 Mpc) to superclusters ($\sim$ 300 Mpc) of galaxies at different instants of their evolution: 400 thousand years after the Big Bang ($E \sim 1$ eV) in the epoch of hydrogen recombination observed in the radio frequency band, and for the modern period of cosmological structure formation ($E \sim 10^{-3}$ eV, 13 billion years after the Big Bang) studied on the basis of the distribution of galaxies and their clusters by optical and X-ray astronomy techniques.

Today we can speak about a qualitative breakthrough in observational cosmology: we know the solution to the problem of the gravitational instability of the Universe. Independently reconstructed were the initial conditions (the primary field of cosmological density perturbations) as well as the values of cosmological model parameters, including the composition and quantity of hidden matter (cold particles, baryons, massive neutrinos) and dark energy (the physical vacuum density), which determine the evolution of density perturbations from the recombination epoch to now.